POLITECNICO
MILANO 1863

SCUOLA DI INGEGNERIA INDUSTRIALE
E DELL'INFORMAZIONE

Executive Summary of the Thesis

Development and characterization of a hybrid time-resolved reflectance spectroscopy and diffuse correlation spectroscopy system for hemodynamic and metabolic measurements

Laurea Magistrale in Engineering Physics – Ingegneria Fisica

Author: Marco Nabacino

Advisor: Prof. Alessandro Torricelli

Co-advisor: Caterina Amendola, PhD

Academic year: 2021-2022

Introduction

The work developed in this thesis concerns the design and characterization of an innovative hybrid time-domain reflectance spectroscopy (TRS) and diffuse correlation spectroscopy (DCS) instrument for hemodynamic and metabolic measurements.
TRS and DCS are diffuse optics techniques that make use of infrared laser light in order to probe biological tissue in a non-invasive manner. More specifically, TRS gives information on the concentration of oxy- and deoxy-hemoglobin and thus tissue oxygen saturation, while DCS allows to quantify blood flow. As such, the combination of the two allows a comprehensive all-optical measurement of tissue oxygenation and hemodynamics. Moreover, a hybrid device allows to measure quantities that each single technique is not able to retrieve on its own with the same degree of accuracy, such as the cerebral metabolic rate of oxygen consumption.

1. Theoretical basis

1.1. Photon migration in tissue

As far as light propagation is concerned, biological tissue falls into the category of *turbid media,* that is, media which both absorb and scatter light propagating through them. Absorption stems from the excitation of molecules in the tissue, while scattering originates from the spatially varying distribution of particle size and refractive index.
The average distance travelled by a photon before being absorbed is called *absorption mean free path;* its reciprocal, denoted by $\mu_a(\lambda)$, is called the *absorption coefficient* and depends on the wavelength of the radiation. Scattering is described similarly by a *scattering mean free path,* the average distance after which a photon undergoes a scattering event, but in this context a longer *transport mean free path* is also used, which represents the average propagation distance travelled by photons before their direction is randomized. Its reciprocal is called the *reduced scattering coefficient* $\mu_s'(\lambda)$.
In biological tissue, scattering dominates over absorption, with typical values of the optical parameters being of order $\mu_a \sim 0.1\,\mathrm{cm}^{-1}$, $\mu_s' \sim 10\,\mathrm{cm}^{-1}$. This condition, known as *diffusion*

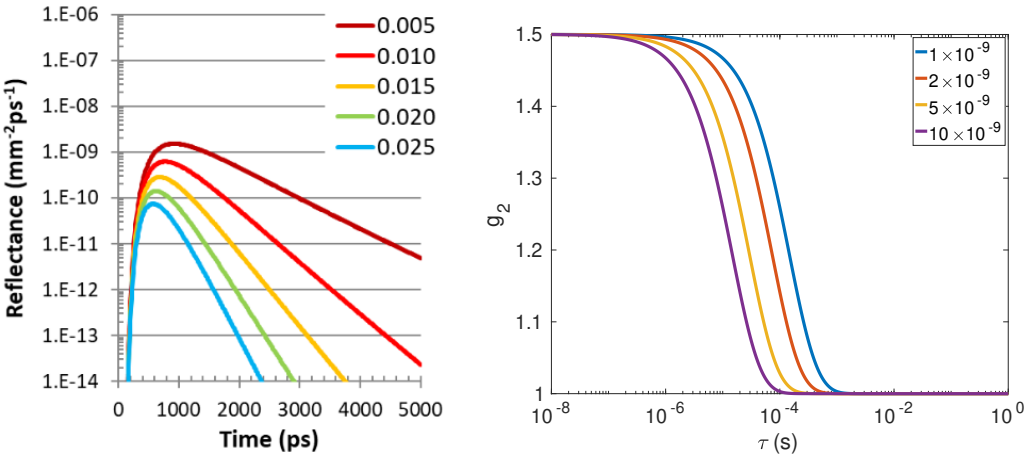

(a) Output pulse shape for different values of μ_a (units mm^{-1})

(b) Autocorrelation function for different values of D_B (units $\mathrm{cm}^2\,\mathrm{s}^{-1}$)

Figure 1: Plots of the theoretical pulse profile in a TRS experiment and autocorrelation function in a DCS experiment according to the diffusion model of photon propagation.

regime, allows to employ the relatively simple diffusion model for describing the phenomenon analytically.

In TRS a pulsed laser source injects light into the tissue, and a detection fiber placed on the same side at distance r away collects the diffused photons. The output pulse is attenuated and delayed, and by fitting its shape with the solution provided by the diffusion model (fig. 1a) the optical parameters μ_a and μ_s' can be retrieved.

1.2. Diffuse correlation spectroscopy

Fluctuations in concentration, density or orientation of molecules give rise to a type of scattering different from the one considered so far. By measuring the fluctuations of the intensity of light scattered by moving particles it is possible to derive information on their motion.

In biological tissue the scatterers are mainly red blood cells, whose motion is well approximated by a Brownian model. Thus, the mean-square displacement of the particles in time τ is equal to $\langle \Delta r^2(\tau) \rangle = 6 D_B \tau$, where D_B is the diffusion coefficient of the Brownian motion.

In a continuous-wave DCS experiment, a constant laser source with high coherence length injects light into the tissue, which is collected by a detection fiber placed at a distance r away. A software or hardware correlator then computes the autocorrelation curve of the detected intensity, and by fitting this function with the theoretical model (fig. 1b) it is possible to retrieve information on the movement of red blood cells in the form of the blood flow index $\mathrm{BFI} = \alpha D_B$, α being the ratio of moving scatterers to total ones.

2. Materials and methods

The overall instrument developed in this thesis is made of two separate setups: a TRS module and a DCS one. Time-domain reflectance spectroscopy allows to retrieve the tissue optical parameters μ_a and μ_s', which are then used by the DCS setup to retrieve the blood flow index. Both modules feature multiple detection channels that work in parallel, allowing to collect light from different points of the investigated sample. This way it is possible to perform measurements at different source-detector separations, which allows to separate the contributions of the superficial layers from those of the deeper tissue.

2.1. TRS setup

TRS is performed thanks to a modified NIRSBOX (PIONIRS s.r.l.), featuring two detectors instead of a single one. The system employs two lasers at different wavelengths, which operate in a time multiplexing scheme in order to avoid cross-talk. Employing two different wavelengths is necessary in order to retrieve the concentrations of both oxy- and deoxy-hemoglobin.

A simplified block scheme of the NIRSBOX is represented in fig. 2a. The light sources are

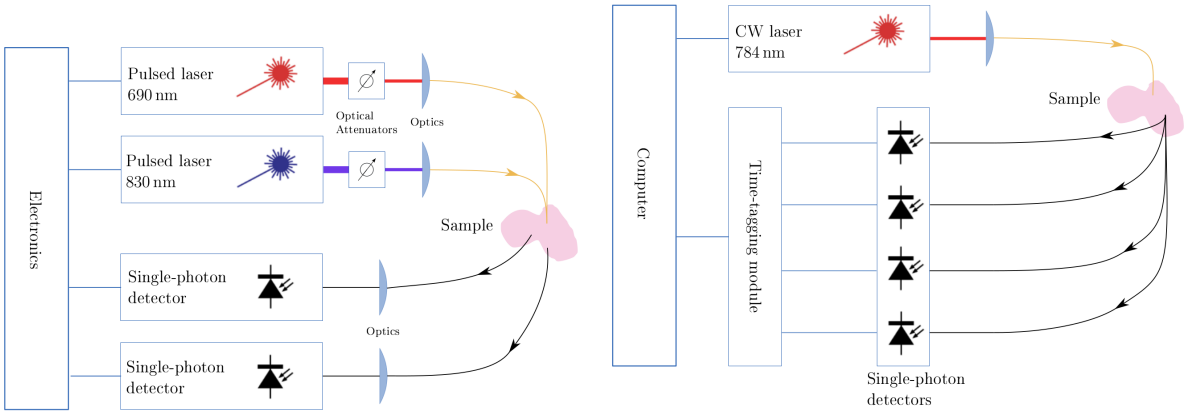

(a) Block scheme of the NIRSBOX (b) Block scheme of the DCS module

Figure 2: Block schemes of the TRS and DCS modules

pulsed-diode lasers, operating in gain-switching mode at 50 MHz, emitting light at 690 nm and 830 nm respectively. The light produced by each source passes through an optical attenuator and is then coupled into a 100 µm graded-index optical fiber. In order to obtain a single injection point, the two input fibers are bundled together. The light scattered by the sample is collected by two graded-index plastic optical fibers with a core diameter of 0.9 mm and detected by two silicon photomultipliers with an active area of $1.3 \times 1.3\ mm^2$. Time-to-digital conversion is performed by an application-specific integrated circuit, allowing reconstruction of the distribution of photon time-of-flight (DTOF).
The instrument is connected to a computer, which controls the NIRSBOX through the homonym software. This allows to adjust the optical attenuators that regulate the output laser power, select the integration time for each iteration as well as visualize the DTOF curves and save the data in real-time.

2.2. DCS setup

A block diagram of the DCS module is represented in fig. 2b. It uses a single CW laser, four single-photon detectors and a time-tagging module (TimeTagger 20 by Swabian Instruments) connected to a PC that calculates the autocorrelation of the incoming photon stream. A software correlator was chosen as opposed to a hardware one, since, albeit fast and easy to use, hardware correlators lack flexibility. On the other hand, software correlators allow pre- and post-processing of the data since they store and operate on the raw photon time-tag stream.
As light source, the DCS modules uses a laser diode emitting at 784 nm with high coherence length (> 8 m). This feature is critical to DCS, since the technique is based on measuring the interference of light diffused by the sample. The light emitted by the laser is coupled into a multimode glass/silica step-index fiber, whose core diameter is 400 µm. The diffused light is collected by four single-mode fibers (core diameter 4.4 µm), which ensure that the coherence of the diffused light is preserved. Four single-photon counting detectors work in parallel to convert the light signal into an electric one. These are silicon avalanche photodiodes with 180 µm active area diameter, characterized by 250 ps temporal resolution and 20 ns dead time. Finally, the multi-channel time tagger allows digital data acquisition.
A C# software was developed in order to control the DCS module. It is capable to switch the laser on and off and to adjust its output power, as well as to calculate the autocorrelation of the diffused light intensity and fit it with the theoretical model to retrieve the diffusion coefficient D_B. Finally, it also allows to visualize the data in real time and save them for post-processing.

3. Phantom measurements

3.1. TRS measurements

The NIRSBOX was characterized in terms of stability, linearity and accuracy. For the stability measurement the DTOF photon counts, barycenter position and FWHM, as well as the

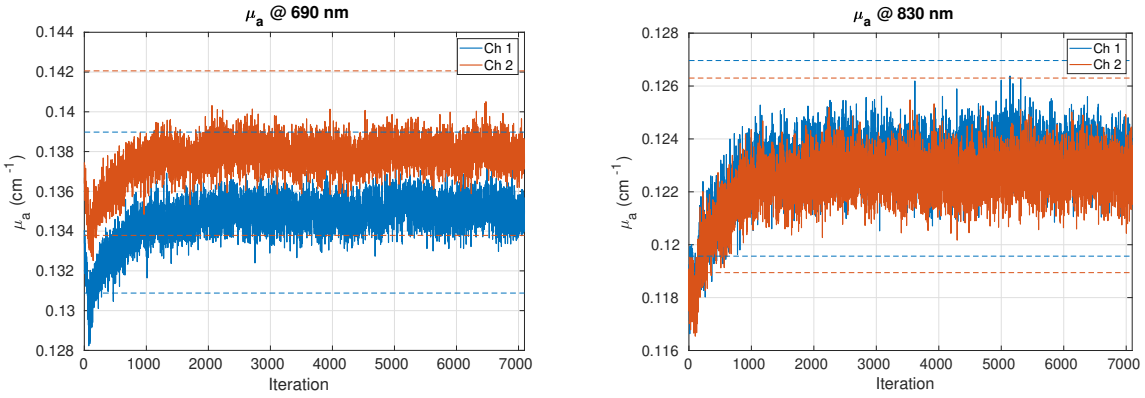

(a) Time evolution of μ_a at $\lambda = 690\,\text{nm}$

(b) Time evolution of μ_a at $\lambda = 830\,\text{nm}$

Figure 3: Temporal evolution of the absorption coefficient as measured by both channels at both wavelengths during the stability measurement. The dashed lines are placed at ±3% of the respective values at regime

retrieved optical parameters were measured for a long time. The goal was to reveal possible short- or long-term drifts of the measurands in time as well as fluctuations, which would be undesirable for clinical applications such as long-time monitoring.

To assess linearity and accuracy, the measured μ_a and μ_s' were compared with the ones yielded by a previously built instrument (a multi-wavelength TRS system used in the PHOOD laboratory). Accuracy is critical for absolute measurements, to ensure that the instrument can retrieve physiological information correctly. Linearity is instead crucial for relative measurements, which means being able to follow variations of such parameters in time without distortions.

The stability, linearity and accuracy of the TRS module were assessed through a set of measurements employing 32 solid phantoms, as prescribed by the MEDPHOT protocol.

For the stability measurement the B3 phantom was chosen, due to its optical parameters resembling those of human tissue ($\mu_s' \simeq 10\,\text{cm}^{-1}$, $\mu_a \simeq 0.14\,\text{cm}^{-1}$). The time evolution of the DTOF photon counts, barycenter and FWHM as well as of the retrieved optical parameters were measured. Figure 3 shows an example of the plots obtained for μ_a. After an initial transitory of about 30 minutes (1000 repetitions) the instrument reaches stability, and the measured quantities stay stationary; the oscillations are within 3% of the mean value for the whole duration. The values of the optical parameters show small discrepancies (less than 2%) at 690 nm, which could be caused by inhomogeneities of the phantom, as well as thermal differences between the two detectors.

To assess the linearity and accuracy of the instrument, a measurement on the full set of MEDPHOT phantoms was carried out and the results were compared to those of the PHOOD instrument (fig. 4). Both detection channels yield compatible values of the absorption and scattering coefficients across all phantoms. For highly absorbing ones (series 5-8) the values of μ_a measured are higher than the ones provided by the other instrument, but they show higher linearity. The phantoms with higher levels of absorption and scattering give bigger error bars on the measurands: this is due to the photons being absorbed or scattered away before reaching the detector, which results in lower signal-to-noise ratios and thus less robust fitting of the curves. The relative errors on both μ_a and μ_s' are very similar between the two detectors at both wavelengths.

3.2. Comparison among autocorrelation algorithms

As for the DCS module, a set of measurements were carried out in order to compare the performance of different methods of calculating the autocorrelation curves. These were a classic multi-tau algorithm which mimics the ones implemented in hardware correlators, an asyn-

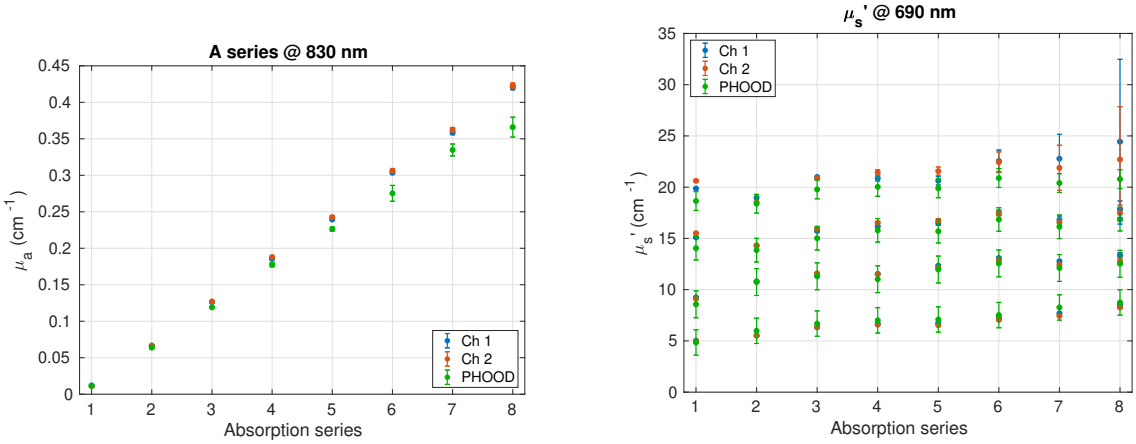

(a) μ_a for the phantoms of the MEDPHOT A series at $\lambda = 690\,\text{nm}$

(b) μ_s' of all phantoms at $\lambda = 690\,\text{nm}$

Figure 4: Example of plots of the values of the optical parameters measured by the NIRSBOX and the PHOOD instrument

chronous algorithm that operates directly on the raw time-tag signal (without performing time-binning beforehand), an FFT-based algorithm that harnesses the Wiener-Khinchin theorem, the algorithm provided by the API of the time-tagger, and a hardware correlator installed on a previously built instrument. The first three algorithms operated in post-processing, while the other calculated the autocorrelation in real-time during the measurements.

The algorithms were compared in terms of speed, stability and ability to follow variations of the autocorrelation curves due to different factors, namely viscosity (to which the diffusion coefficient D_B is inversely proportional according to the Einstein relation) and inter-fiber distance. Figure 5a shows an example of the curves obtained with the different algorithms. They all exhibit approximately the same decay, but different levels of noise, with the noisiest being the time-tagger one. The FFT curve has many more data points than the other ones, and they become denser on the logarithmic axis for higher values of the time delay. This is due to the linearly spaced values of τ used by the FFT algorithm.

As for time performance, the asynchronous algorithm proved to be the fastest one, taking about $0.6 \div 1.0$ s per curve for a count rate of 150 kHz. The FFT-based algorithm took $5 \div 7$ s, and the classic multi-tau one $150 \div 180$ s. Note that the ratios between these values is significant rather than their absolute values, since the latter strongly depend on the computational power of the PC used.

The stability measurement showed that the autocorrelation provided by the time-tagger has the highest variability, with an error on D_B spanning one order of magnitude (fig. 5b). The other algorithms show errors below 5%, except for the FFT-based one, which has a coefficient of variation of about 12%. This is likely due to the difficulty in finding the right fitting interval for its curve, because of the linearity of time bins and abundance of data points. As for accuracy, the time-tagger algorithm yields a mean value of D_B much higher than the other ones, which are all compatible.

In the second set of measurements four different phantoms were employed, each one containing a different concentration of glycerol. Glycerol affects the viscosity of the solution, so that higher concentrations produce higher viscosities and thus lower values of D_B. This decrease is detected by all algorithms except for the time-tagger one, which on top of exhibiting high variability (up to 500%) is also wildly inaccurate at times, yielding values of D_B that are up to one order of magnitude greater than the others. The FFT algorithm shows relatively high variability ($10\% \div 30\%$), while the other ones are around 5%.

Finally, a measurement at variable inter-fiber distance was performed in order to test how well

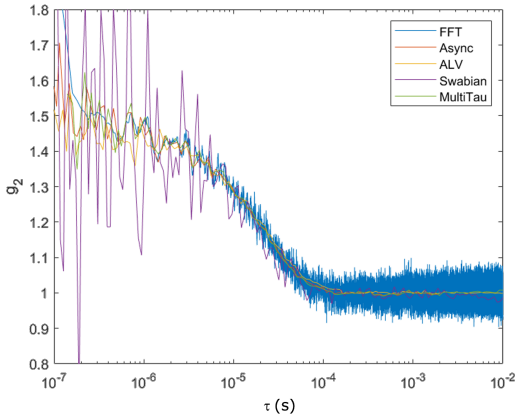

(a) Autocorrelation curves calculated by the various algorithms

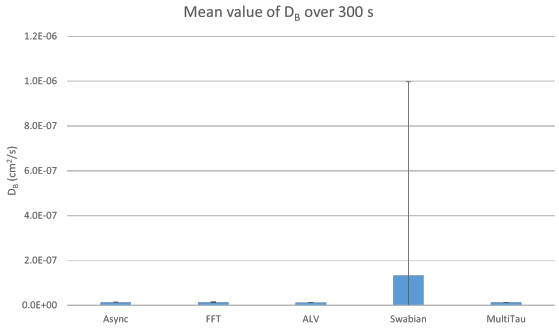

(b) Mean value of D_B yielded by the different algorithms in the stability measurement

Figure 5: Examples of plots comparing the different autocorrelations algorithms

the different algorithms could detect the effect of source-detector separation on the correlation curve. Again, the time-tagger algorithm exhibits high variability and on top of this overestimates D_B by one order of magnitude at short inter-fiber distance (1 cm). The asynchronous, hardware and multi-tau correlations all agree on the value of D_B, while the FFT algorithm yields a higher value.

4. Conclusions

This thesis work focused on the development and characterization of an innovative compact instrument for hemodynamic and metabolic measurements. The device employs non-invasive diffuse-optics techniques, namely TRS and DCS. The TRS module was assessed in terms of stability, linearity and accuracy. The stability measurement showed that the instrument reaches a stationary regime in 30 minutes, and the oscillations of the optical parameters always stay within 3% of their mean value. The linearity and accuracy measurements validated the device against a previously built one, showing that the developed device is suitable for both absolute and relative measurements.
Differently from previously built systems, the DCS module employs a software autocorrelator: several algorithms were compared in terms of stability as well as capability of following variations in sample viscosity and source-detector separation. The experiments showed that, although very fast, the time-tagger algorithm is both inaccurate and extremely imprecise, making it a poor choice for anything but a qualitative visualization of the data during the measurement. On the other hand, the asynchronous multi-tau algorithm that was tested showed performance comparable to that of hardware correlators while still keeping computational time low. This makes it a great choice for analyzing the data not only in post-processing, but potentially in real-time too.

References

[1] Caterina Amendola et al. "A Compact Multi-Distance DCS and Time Domain NIRS Hybrid System for Hemodynamic and Metabolic Measurements". In: *Sensors* 21.3 (2021). DOI: 10.3390/s21030870.

[2] T. Durduran et al. "Diffuse optics for tissue monitoring and tomography". In: *Reports on Progress in Physics* 73.7 (June 2010), p. 076701. DOI: 10.1088/0034-4885/73/7/076701.

[3] Michele Lacerenza et al. "Wearable and wireless time-domain near-infrared spectroscopy system for brain and muscle hemodynamic monitoring". In: *Biomed. Opt. Express* 11.10 (Oct. 2020), pp. 5934–5949. DOI: 10.1364/BOE.403327.

[4] Antonio Pifferi et al. "Performance assessment of photon migration instruments: the MEDPHOT protocol". In: *Appl. Opt.* 44.11 (Apr. 2005), pp. 2104–2114. DOI: 10.1364/AO.44.002104.